(45 mL) at 23 °C. The clear yellow reaction mixture was stirred for 4 h, and a precipitate formed. Removal of all volatile materials under vacuum and subsequent washing of the yellow residue with *n*-pentane (2 × 30 mL) yielded, after drying, powdery white **4** (1.32 g, 1.74 mmol, 83 %); m.p. 190 °C (decomp.). Elemental analysis calcd for $C_{18}H_{30}MgN_2O_3S$: C 57.07, H 7.98, N 7.40; found: C 57.35, H 7.77, N 7.59; ^{1}H NMR ([D$_8$]THF, 23 °C): 7.23 (br, 2H, *o*-H), 6.86 (m, 2H, *m*-H), 6.33 (m, 1H, *p*-H), 3.58 (m, 8H, $(CH_2)_2(CH_2)_2O$), 1.74 (m, 8H, $(CH_2)_2(CH_2)_2O$), 1.34 (s, 9H, $C(CH_3)_3$); ^{13}C{^{1}H} NMR ([D$_8$]THF, 23 °C): 154.0 (s, *ipso*-C), 128.4 (s, *o*-C), 115.0 (s, *m*-C), 96.8 (s, *p*-C), 67.9 (s, $(CH_2)_2(CH_2)_2O$), 52.4 (s, $C(CH_3)_3$), 34.3 (s, $C(CH_3)_3$), 26.4 (s, $(CH_2)_2(CH_2)_2O$).

Received: October 4, 1999
Revised: December 2, 1999 [Z14096]

[1] a) W. Kitching, C. W. Fong, *Organomet. Chem. Rev. A* **1970**, *5*, 281; b) A. Wojicki, *Adv. Organomet. Chem.* **1974**, *12*, 32; c) S. L. Livingstone in *Comprehensive Coordination Chemistry*, *Vol. 2* (Eds.: G. Wilkinson, R. G. Gillard, J. A. McLeverty), Pergamon, Oxford, **1987**, p. 190; d) A. F. Hill, *Adv. Organomet. Chem.* **1994**, *36*, 159.
[2] D. Masilamani, M. M. Rogic, *J. Am. Chem. Soc.* **1978**, *100*, 4634.
[3] V.-C. Arunasalam, I. Baxter, M. B. Hursthouse, K. M. A. Malik, D. M. P. Mingos, J. C. Plakatouras, *J. Chem. Soc. Chem. Commun.* **1994**, 2695.
[4] T. A. George, K. Jones, M. F. Lappert, *J. Chem. Soc.* **1965**, 2157.
[5] a) D. E. Wigley, *Prog. Inorg. Chem.* **1994**, *42*, 239; b) P. Mountford, *Chem. Commun.* **1997**, 2127.
[6] a) T. Hascall, K. Ruhlandt-Senge, P. P. Power, *Angew. Chem.* **1994**, *106*, 350; *Angew. Chem. Int. Ed. Engl.* **1994**, *33*, 356; b) M. M. Olmstead, W. J. Grigsby, D. R. Chacon, T. Hascall, P. P. Power, *Inorg. Chim. Acta* **1996**, *251*, 273; c) W. J. Grigsby, M. M. Olmstead, P. P. Power, *J. Organomet. Chem.* **1996**, *513*, 173; d) W. J. Grigsby, T. Hascall, J. J. Ellison, M. M. Olmstead, P. P. Power, *Inorg. Chem.* **1996**, *35*, 3254.
[7] a) M. Veith, *Coord. Chem. Rev.* **1990**, *90*, 1; b) M. Veith, *Angew. Chem.* **1987**, *99*, 1; *Angew. Chem. Int. Ed. Engl.* **1987**, *26*, 1.
[8] a) M. A. Beswick, D. S. Wright, *Coord. Chem. Rev.* **1998**, *176*, 373; b) R. E. Allan, M. A. Beswick, N. L. Cromhout, M. A. Paver, P. R. Raithby, A. Steiner, M. Trevithick, D. S. Wright, *Chem. Commun.* **1996**, 1501.
[9] a) Crystal data for **2**: $C_{10}H_{13}NO_5S_2Mg \cdot C_4H_8O$, $M_r = 387.75$, trigonal/hexagonal, space group $R\bar{1}$ (no. 148), $a = 26.871(4)$, $c = 13.506(10)$ Å, $V = 8446(6)$ Å^3, $Z = 18$, $\rho_{calcd} = 1.372$ g cm^{-3}, $\mu(Mo_{K\alpha}) = 0.345$ mm^{-1}, $\lambda(Mo_{K\alpha}) = 0.71069$ Å, $T = -103$ °C, $F(000) = 3672$. Data were collected on a Rigaku AFC6S diffractometer on a pale yellow needle (0.42 × 0.19 × 0.18 mm) coated with Paratone-8277 oil and mounted on a glass fiber by the $\omega/2\theta$ scan method. Of the 2725 reflections collected, 2551 were unique ($R_{int} = 0.221$), and 469 were observed [$I > 2\sigma(I)$] and used to refine 101 parameters. The structure was solved by direct methods (SIR92), expanded with Fourier techniques (DIRDIF94) and refined by SHELXL97. The Mg and S atoms were refined anisotropically, and the rest of the non-hydrogen atoms were refined isotropically. The phenyl ring and THF molecules were included with constrained geometry. Hydrogen atoms were included but not refined. Refinement by full-matrix least-squares calculations converged at $R = 0.127$ and $R_w = 0.325$. Numerous attempts to obtain better quality crystals of **2** were unsuccessful. b) Crystallographic data (excluding structure factors) for the structures reported in this paper have been deposited with the Cambridge Crystallographic Data Centre as supplementary publications no. CCDC-135289 (**2**) and -135290 (**4**). Copies of the data can be obtained free of charge on application to CCDC, 12 Union Road, Cambridge CB2 1EZ, UK (fax: (+44) 1223-336-033; e-mail: deposit@ccdc.cam.ac.uk).
[10] The isoelectronic disulfite dianion $[O_2S{-}SO_3]^{2-}$ contains an S–S bond: N. N. Greenwood, A. Earnshaw, *Chemistry of the Elements*, 2nd ed., Butterworth-Heinemann, Oxford, UK, **1997**, p. 720.
[11] For examples of other inorganic complexes involving fused adamantane-like units, see a) W. Hirpo, S. Dhingra, M. G. Kanatzidis, *J. Chem. Soc. Chem. Commun.* **1992**, 557; b) B. Krebs, G. Henkel, *Angew. Chem.* **1991**, *103*, 785; *Angew. Chem. Int. Ed. Engl.* **1991**, *30*, 769; c) I. Dance, *Polyhedron* **1986**, *5*, 1037.
[12] Crystal data for **4**: $C_{18}H_{30}N_2O_3SMg \cdot C_4H_8O$, $M_r = 450.92$, triclinic, space group $P\bar{1}$ (no. 2), $a = 11.8785(19)$, $b = 12.514(3)$, $c = 9.033(2)$ Å, $\alpha = 104.91(2)$, $\beta = 93.880(19)$, $\gamma = 71.223(16)^\circ$, $V = 1228.3(5)$ Å^3, $Z = 2$, $\rho_{calcd} = 1.219$ g cm^{-3}, $\mu(Mo_{K\alpha}) = 0.177$ mm^{-1}, $\lambda(Mo_{K\alpha}) = 0.71069$ Å, $T = -103$ °C, $F(000) = 488$. A colorless hexagonal prism (0.53 × 0.33 × 0.29 mm) was coated with Paratone-8277 oil and mounted on a glass fiber. Of the 4565 reflections collected, 4337 were unique ($R_{int} = 0.042$), and 2087 were observed [$I > 3\sigma(I)$] and used to refine 271 parameters. The structure was solved by direct methods and expanded with Fourier techniques. The non-hydrogen atoms were refined anisotropically. Hydrogen atoms were included at geometrically idealized positions and were not refined. Refinement by full-matrix least-squares calculations converged at $R = 0.055$ and $R_w = 0.057$.[9b]
[13] J. K. Brask, T. Chivers, M. Parvez, G. Schatte, *Angew. Chem.* **1997**, *109*, 2075; *Angew. Chem. Int. Ed. Engl.* **1997**, *36*, 1986.
[14] A. J. Edwards, M. A. Paver, P. R. Raithby, M.-A. Rennie, C. A. Russell, D. S. Wright, *Angew. Chem.* **1994**, *106*, 1334; *Angew. Chem. Int. Ed. Engl.* **1994**, *33*, 1277.
[15] J. K. Brask, T. Chivers, B. McGarvey, G. Schatte, R. Sung, R. T. Boeré, *Inorg. Chem.* **1998**, *37*, 4633.
[16] G. Kresze, A. Maschke, R. Albrecht, K. Bederke, H. P. Patzschke, H. Smalla, A. Trede, *Angew. Chem.* **1962**, *74*, 135; *Angew. Chem. Int. Ed. Engl.* **1962**, *1*, 89.

Controllable Orientation of Helical Poly(L-glutamic acid) Rods through Macrodipole Interaction on Gold Surfaces and Vectorial Electron Transfer

Masazo Niwa,* Masa-aki Morikawa, and Nobuyuki Higashi*

Helix orientation at interfaces is one of the key factors to fabricate biofunctional synthetic polymer systems that mimic natural polymers such as proteins. The orientation of segments in membrane proteins is known to govern functions such as molecular recognition and electrochemical communication, including electron transfer. In this context, there has been considerable interest in constructing perpendicularly oriented polypeptide monolayers on aqueous or solid substrates. It has been indicated that α helices prefer to lie flat on every possible interface.[1] Efforts have been made to orient α helices perpendicular to the surface of the water or solid substrates,[2–5] by incorporation of functional groups onto one terminus of polypeptide helices. Such groups under consideration include quaternary ammonium groups[6, 7] to interact with anionic templates, a crown ether moiety,[8–10] or a sulfur atom[11–14] to attach to a gold surface.

In this communication, we describe the reversible variation of the orientation of a disulfide-modified poly(L-glutamic acid) (PLGA-SS) α helix assemblies attached to a gold surface and their enhanced molecular packing based on the interaction of helix macroscopic dipoles ("macrodipoles"). We

[*] Prof. M. Niwa, Prof. N. Higashi, M.-a. Morikawa
Department of Molecular Science & Technology
Doshisha University
Kyo-tanabe, Kyoto 610-0321 (Japan)
Fax: (+81) 774-65-6844
E-mail: mniwa@mail.doshisha.ac.jp, nhigashi@mail.doshisha.ac.jp

  0570-0833/00/3905-0960 $ 17.50+.50/0

have investigated the macrodipole-induced formation of aggregates of α helical polypeptides on water[15] and gold substrates.[13a] The macrodipole of helical polypeptides, resulting from the accumulation of dipole moments of the component peptide bonds, produces an electrostatic potential directed from the N-terminus to the C-terminus.[16, 17] Such an electrostatic potential plays an important role in the higher-order structures and functions of proteins.[18–20] Fox et al.[21, 22] have demonstrated that the macrodipole influences the efficiency of photoinduced, intramolecular fluorescence quenching. In our previous report,[13b] we have provided a direct evidence for helix–helix macrodipole interaction by exploring an attractive interaction between the PLGA-SS monolayers on gold and redox-active PLGA derivatives (PLGA-Fc-N and PLGA-Fc-C) as "guest" helices (Figure 1). Now we report on the extension of this PLGA-helix system to the control of the orientation and molecular packing of the helix monolayers and also on mediator functions of the redox-active guest helices.

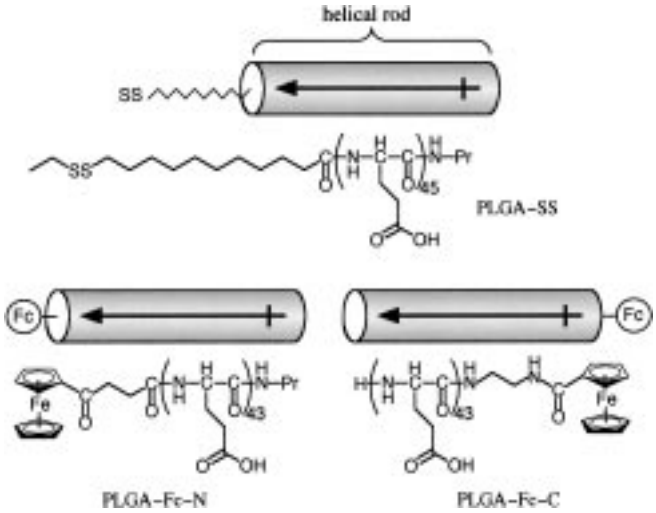

Figure 1. Molecular structures for the monolayer-forming PLGA disulfide derivative (PLGA-SS) and the ferrocenyl-modified, redox-active PLGA guests (PLGA-Fc-N, PLGA-Fc-C) used in this study. The corresponding schematic models of the helical rods are also shown. Arrows indicate the moment of the helix macrodipole.

We have previously developed a technique[13b] for the lateral molecular distribution of PLGA-SS onto a gold surface. By such a technique, the molecular packing within the resulting monolayer can be readily varied by adjusting the conformational size of the PLGA segments through the solution pH.

To examine the orientation of helical rods, two kinds of self-assembled monolayers of PLGA-SS were prepared on gold substrates: one of them is the densely packed monolayer prepared at pH 4.5, in which the PLGA segments take a α helix structure (monolayer **I**); the other is the more loosely packed monolayer prepared at pH 9.0, in which the PLGA segments take an expanded coil conformation (monolayer **II**). After reaching adsorption equilibrium, both of the monolayers were immersed into water at pH 3.5 to convert the conformation of the PLGA segments completely to the α helix structure. In addition, as previously reported, monolayer **II** has suitable cavities for accepting guest PLGA helices (PLGA-Fc-N or PLGA-Fc-C).[13b] Figures 2a and 2b display

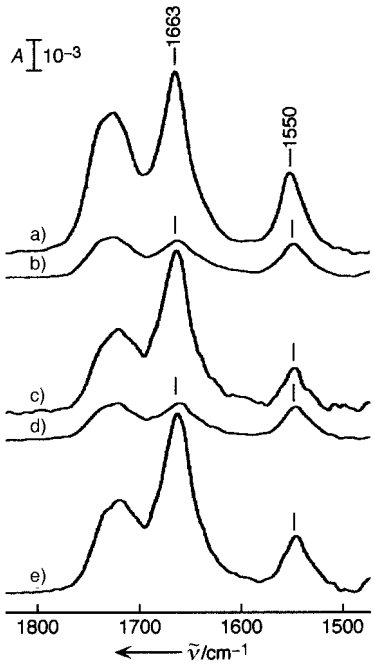

Figure 2. RA-FTIR spectra of the PLGA-SS monolayers: a) prepared at pH 4.5 and then treated with water of pH 3.5 (monolayer **I**); b) prepared at pH 9.0 and then treated with water of pH 3.5 (monolayer **II**); c) monolayer **II** complexed with PLGA-Fc-N; d) monolayer **II** after desorption of PLGA-Fc-N; and e) monolayer **II** re-complexed with PLGA-Fc-C.

reflection–absorption (RA) FTIR spectra of the C=O stretching region for monolayers **I** and **II**, respectively. The differences in absorption are remarkable, reflecting differences in surface coverage. In the amide I and amide II regions (1700–1500 cm^{-1}), both spectra exhibit two bands at 1663 and 1550 cm^{-1}, which are assigned to the α helix structure.[23, 24] The additional C=O stretching band, due to COOH groups of the side chain of PLGA, is observed at 1730 cm^{-1}. Enriquez et al.[25] demonstrated that the nature of the order and average orientation of the polypeptide α helix in the films can be inferred from RA-FTIR data. By using the ratio of the integrated intensities of the amide I and amide II regions, $D = A_I/A_{II}$, the average tilt of the helix axis from the surface normal, $\langle\theta\rangle$,[26] was evaluated to be 40° and 51° for monolayers **I** and **II**, respectively (Table 1). Such a difference in the tilting angle can be reasonably interpreted by accounting for the

Table 1. Ratio D of the integrated intensities of the amide I to amide II regions from RA-FTIR spectra and the average tilt angle of the helix axes from the surface normal ($\langle\theta\rangle$).[a]

System	D	$\langle\theta\rangle$ [°]
monolayer **I**	2.8	40 ± 3
monolayer **II**	1.7	51 ± 3
monolayer **II** with PLGA-Fc-N	5.8	25 ± 3
monolayer **II** without PLGA-Fc-N	1.5	55 ± 3
monolayer **II** with PLGA-Fc-C	5.2	27 ± 3

[a] The $\langle\theta\rangle$ values were estimated from the D values,[26] with $\tilde{\nu}$(amide I) = 1663, $\tilde{\nu}$(amide II) = 1550 cm^{-1}. Details are described in the text.

  0570-0833/00/3905-0961 $ 17.50+.50/0

molecular packing density in the monolayers; for the more densely packed monolayer **I**, the helices are obliged to orient more perpendicularly to the surface due to crowding with the helical rods in comparison to the less densely packed monolayer **II**. The rigid PLGA-SS helical rods, anchored to the gold surface through a flexible methylene spacer, will lie as flat as possible on the substrate, as observed for the loosely packed monolayer **II**. It should be noted that also the helices of monolayer **I** are tilted from the surface normal in spite of their high packing density. In this monolayer, the helices must be assembled into a parallel packing. These helical peptides are known to carry a macrodipole moment along the helix axis.[15] Thus, a parallel packing of the helices is energetically unfavorable, and as a result the helical rods in monolayer **I** achieve a tilting angle of 40° to compensate for such an energetic disadvantage.

Figure 2c shows the RA-FTIR spectrum of monolayer **II** after complexation with PLGA-Fc-N. In the previous study,[13b] we demonstrated that monolayer **II** is able to accept both PLGA-Fc-N and -C guests at a 1:1 composition through macrodipole interaction. From the value of the ratio *D*, the tilting angle of the helices is calculated to be 25° (Table 1), which is significantly enhanced in the perpendicular orientation of helical rods, compared with the 51° tilt found before complexation. This result suggests that by complexation of monolayer **II** with the PLGA-Fc-N helix, a monolayer in a head-to-tail antiparallel orientation, which is energetically more favorable, is spontaneously formed, and consequently achieves a nearly perpendicular helix orientation. This effect is shown schematically in Figure 3a and 3b. When this complexed monolayer was treated with water at pH 9.0, the PLGA segments underwent a conformational change from α helix to random coil, then the monolayer released the guest PLGA-Fc-N into the bulk aqueous phase because of the loss of the helix macrodipole. An RA-FTIR spectrum of the monolayer after the pH-induced desorption of PLGA-Fc-N is similar to the original monolayer (Figure 2d and 2b), and consequently the tilting angle returns to the original value of monolayer **II** (Table 1). The spectrum of Figure 2e arises when the other guest, PLGA-Fc-C, is incorporated into monolayer **II**. The calculated tilting angle of the helices (Table 1) again approaches the perpendicular orientation.

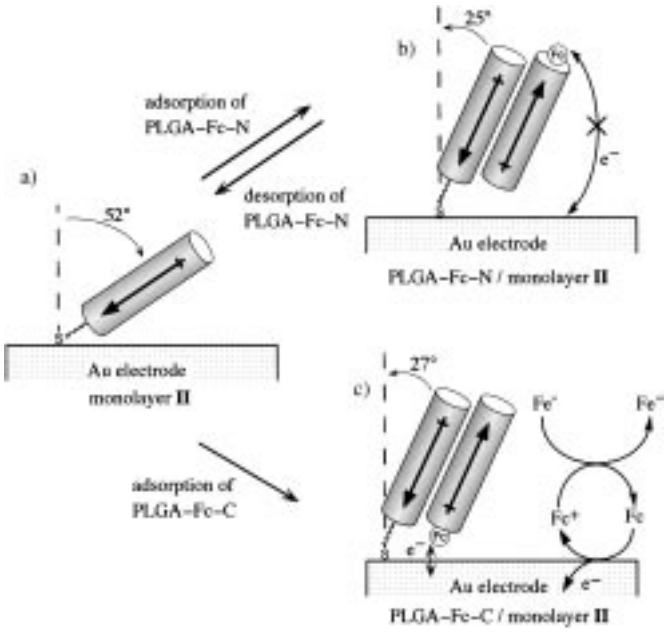

Figure 3. Illustration of the proposed mechanism for the reversible variations in PLGA helix rod orientation upon adsorption and desorption of guest helices and for the electron mediation function of the ferrocenyl moiety on gold substrates: a) pure monolayer **II**; b) monolayer **II** complexed with PLGA-Fc-N; and c) monolayer **II** complexed with PLGA-Fc-C.

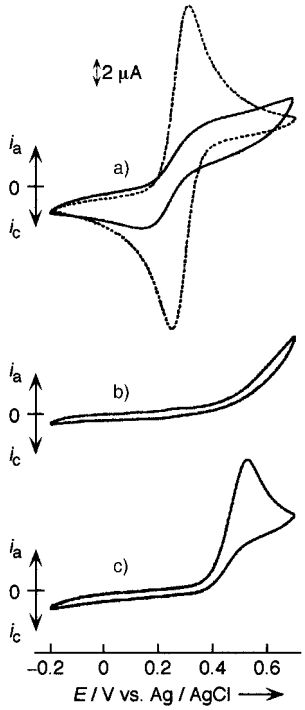

Figure 4. Cyclic voltammograms of gold electrodes modified with monolayer **II** in the presence of 3 mM $[Fe(CN)_6]^{4-}$ (scan rate 100 mV s^{-1}): a) bare gold electrode (----) and monolayer **II** (——); b) after complexation with PLGA-Fc-N; and c) after complexation with PLGA-Fc-C.

The molecular packing of these monolayers before and after binding of the guest PLGAs was subsequently evaluated as an electrochemical barrier toward the redox couple of $[Fe(CN)_6]^{3-}$/$[Fe(CN)_6]^{4-}$. Figure 4a shows a cyclic voltammogram (CV) for the gold surface (electrode) modified with monolayer **II**, in comparison with that for a bare electrode. The peaks due to the redox reaction of $Fe^{III} \leftrightarrow Fe^{II} + e^-$ are observed but their peak currents are considerably suppressed in comparison with those of the bare electrode. This implies that a monolayer was formed while having a void for the probe ion to diffuse to the electrode surface. When this electrode was immersed into an aqueous solution with PLGA-Fc-N at pH 3.5 to adsorption equilibrium, the peaks for the $Fe^{III} \leftrightarrow Fe^{II} + e^-$ reaction were found to disappear completely (Figure 4b), indicating that the electrochemical blocking ability of the monolayer was markedly enhanced because of binding of the PLGA-Fc-N guest, which has the ferrocenyl moiety at the N-terminus which is, by the macrodipole interaction, oriented away from the surface. Figure 4c displays a CV curve after binding of the guest PLGA-Fc-C, which has the ferrocenyl moiety at the C-terminus which is oriented towards the surface. In this case, there is also no peak that corresponds to the redox reaction of $Fe^{III} \leftrightarrow Fe^{II} + e^-$, reflecting the same blocking ability as observed for the electrode bound with the PLGA-Fc-N monolayer. As reported previously,[13b] when the CV analysis had been performed for this electrode covered with a PLGA-Fc-C monolayer under the same conditions except for absence of $[Fe(CN)_6]^{4-}$, two peaks had appeared at around +0.5 V (vs. Ag/AgCl) due to one-electron oxidation and reduction of the ferrocenyl moiety of the bound PLGA-Fc-C. Furthermore, the peak current (*i*) acquired at different potential scan rates

  0570-0833/00/3905-0962 $ 17.50+.50/0 *Angew. Chem. Int. Ed.* **2000**, *39*, No. 5

(v) was found to vary linearly with the scan rate, indicating that PLGA-Fc-C was bound to the monolayer **II** and not subject to diffusion to the electrode. In the presence of $[Fe(CN)_6]^{4-}$ there appears, however, an oxidation peak for the ferrocenyl moiety at around +0.5 V (vs. Ag/AgCl), with a remarkably large current compared with that observed in the absence of $[Fe(CN)_6]^{4-}$ at the same scan rate, and no reduction peak was observed. This electrode, when the scan rate was varied at a constant concentration of $[Fe(CN)_6]^{4-}$ (3 mM), yields a linear i versus $v^{1/2}$ plot, to show the catalyzed reaction is sufficiently fast such that the process is controlled by $[Fe(CN)_6]^{4-}$ diffusion.[28] From these results, it can be assumed that the immobilized ferrocenyl moiety facing the electrode surface behaves successfully as an electron-transfer mediator and the direction of electron transfer must be vectorial as schematically illustrated in Figure 3. To further support this hypothesis, the dependence on the $[Fe(CN)_6]^{4-}$ concentration was examined under conditions similar to those in Figure 4c (data not shown). The oxidation peak of the ferrocenyl moiety grew upon increasing the concentration of $[Fe(CN)_6]^{4-}$, as expected for a mediated process.[29]

In conclusion, the orientation of helix rods and the precise location of a redox moiety in self-assembled monolayers have been demonstrated to be controlled through the helix–helix macrodipole interaction. The presented polypeptide assembly system must be a useful model of electron-transfer functions in cell membranes.

Experimental Section

Materials: poly(L-glutamic acid) derivatives PLGA-SS, PLGA-Fc-N, and PLGA-Fc-C were prepared as previously described[13b] and characterized by MALDI-TOF (matrix-assisted laser desorption ionization time-of-flight) mass spectrometry.

Fabrication of PLGA-SS-modified surfaces: A gold disk electrode (BAS, surface 0.02 cm^2) was cleaned by sonication in a 0.1 M aqueous KOH solution for a few minutes, careful polishing with diamond and alumina pastes (mean particle sizes 1 μm and 0.05 μm, respectively), and rinsing with Milli-Q purified water. Gold substrates, on clean glass slides, used for RA-FTIR were prepared by thermal evaporation of gold at a pressure of ca. 10^{-6} Torr and cleaned by rinsing with $CHCl_3$ and Milli-Q water prior to use. The monolayers were prepared by immersing the gold substrates into aqueous solutions containing PLGA-SS (1 mM) at pH 4.5 or pH 9.0 until adsorption equilibrium was reached, followed by incubating in water (pH 3.5).

Measurements: Cyclic voltammetry was performed at 25 °C with a CV-1B cyclic voltammograph (BAS). A standard three-electrode configuration was used with the monolayer sample on gold as the working electrode, Ag/AgCl (3 M NaCl) as the reference electrode, and a platinum wire as the counter electrode. $K_4[Fe(CN)_6]$ was obtained commercially and used as received. The solutions containing 1 M KCl as a supporting electrolyte were deoxygenated by an N_2 purge. FTIR was performed on a Nicolet System 800 spectrometer with a mercury-cadmium-tellurium (MCT) detector. The RA-FTIR measurements used 1024 scans of interferogram accumulations with the bare gold substrate as reference. The optical path was purged with dry air before and during measurements. A reflection attachment, at an incident angle of 80°, together with a polarizer was used.

Received: July 7, 1999
Revised: October 19, 1999 [Z13690]

[1] J. Stumpe, T. Fischer, H. Menzel, *Macromolecules* **1996**, *29*, 2831.
[2] J. K. Whitesell, H. K. Chang, *Science* **1993**, *261*, 73.
[3] A. E. Strong, B. D. Moore, *Chem. Commun.* **1998**, 473.
[4] Y.-C. Chang, C. W. Frank, *Langmuir* **1996**, *12*, 5824.
[5] M. Boncheva, H. Vogel, *Biophys. J.* **1997**, *73*, 1056.
[6] M. Niwa, T. Takada, N. Higashi, *J. Mater. Chem.* **1998**, *8*, 633.
[7] K. Kishihara, T. Kinoshita, T. Mori, Y. Okahata, *Chem. Lett.* **1998**, 951.
[8] H. Hosokawa, T. Kinoshita, Y. Tsujita, H. Yoshimizu, *Chem. Lett.* **1997**, 745.
[9] Y. Miura, S. Kimura, Y. Imanishi, J. Umemura, *Langmuir* **1998**, *14*, 2761.
[10] Y. Miura, S. Kimura, Y. Imanishi, J. Umemura, *Langmuir* **1999**, *15*, 1155.
[11] C. G. Worley, R. W. Linton, E. T. Samulski, *Langmuir* **1995**, *11*, 3805.
[12] K. Fujita, N. Bunjes, K. Nakajima, M. Hara, H. Sasabe, W. Knoll, *Langmuir* **1998**, *14*, 6167.
[13] a) M. Niwa, T. Murata, M. Kitamatsu, T. Matsumoto, N. Higashi, *J. Mater. Chem.* **1999**, *9*, 343; b) M. Niwa, M. Morikawa, N. Higashi, *Langmuir* **1999**, *15*, 5088.
[14] a) E. Katz, V. Hegel-Shabtai, I. Willner, H. K. Rau, W. Haehnel, *Angew. Chem.* **1998**, *110*, 3443; *Angew. Chem. Int. Ed.* **1998**, *37*, 3253; b) I. Willner, V. Hegel-Shabtai, E. Katz, H. K. Rau, W. Haehnel, *J. Am. Chem. Soc.* **1999**, *121*, 6455.
[15] N. Higashi, M. Sunada, M. Niwa, *Langmuir* **1995**, *11*, 1864.
[16] A. Wada, *Adv. Biophys.* **1976**, *9*, 1.
[17] W. G. J. Hol, P. T. van Duijnen, H. J. C. Berendsen, *Nature* **1978**, *273*, 443.
[18] R. Fairman, K. R. Shoemaker, E. J. York, J. M. Stewart, R. L. Baldwin, *Proteins* **1989**, *5*, 1.
[19] A. Chakrabartty, A. J. Doig, R. L. Baldwin, *Proc. Natl. Acad. Sci. USA* **1993**, *90*, 11332.
[20] K. M. Armstrong, R. L. Baldwin, *Proc. Natl. Acad. Sci. USA* **1993**, *90*, 11337.
[21] T. L. Batchelder, R. J. Fox III, M. S. Meier, M. A. Fox, *J. Org. Chem.* **1996**, *61*, 4206.
[22] M. A. Fox, E. Galoppini, *J. Am. Chem. Soc.* **1997**, *119*, 5277.
[23] T. Miyazawa, E. R. Blout, *J. Am. Chem. Soc.* **1961**, *83*, 712.
[24] K. Kurihara, T. Abe, N. Higashi, M. Niwa, *Colloids Surf. A* **1995**, *103*, 265.
[25] E. P. Enriquez, E. T. Samulski, *Mater. Res. Soc. Symp. Proc.* **1992**, *255*, 423.
[26] The calculations of the tilt angles have been carried out by using Equation (1), proposed by Enriquenz et al.[25]; where the angles of the transition moment (amide I and amide II) from the helix axis are supposed as 39° and 75°, respectively,[27] and K is a proportionality constant that relates the intrinsic oscillator strengths of the amide I and amide II vibrational modes. The value of K has been calculated for LB films of PBLG to be 1.5 ± 0.2.

$$D\left(=\frac{A_{\mathrm{I}}}{A_{\mathrm{II}}}\right) = K\frac{\frac{1}{2}(\sin\langle\theta\rangle\sin 39)^2 + (\cos\langle\theta\rangle\cos 39)^2}{\frac{1}{2}(\sin\langle\theta\rangle\sin 75)^2 + (\cos\langle\theta\rangle\cos 75)^2} \quad (1)$$

[27] M. Tsuboi, *J. Polym. Sci.* **1965**, *59*, 139.
[28] J. E. Hutchison, T. A. Postlethwaite, R. W. Murray, *Langmuir* **1993**, *9*, 3277.
[29] K. S. Alleman, K. Weber, S. E. Creager, *J. Phys. Chem.* **1996**, *100*, 17050.

  0570-0833/00/3905-0963 $ 17.50+.50/0